J Solid State Electrochem (2005) 9: 320–329
DOI 10.1007/s10008-004-0602-1

ORIGINAL PAPER

Edoardo Guerrini · Valerio Consonni · Sergio Trasatti

Surface and electrocatalytic properties of well-defined and vicinal RuO_2 single crystal faces

Received: 1 September 2004 / Revised: 5 October 2004 / Accepted: 6 October 2004 / Published online: 21 January 2005

Abstract The kinetics of Cl_2 evolution from concentrated NaCl solutions on the (110) and (230) faces of RuO_2 single crystals has been investigated by determining the Tafel slope, the stoichiometric number and the reaction orders with respect to Cl^- and H^+. The experimental parameters suggest that the mechanism is presumably similar to that put forward earlier by Krishtalik [51] for RuO_2 layers, but a step common to oxygen evolution, like the case of polycrystalline samples, is present only with the (230) face. Reasons for this difference and for the apparent lower activity of the (110) face with respect to the (230) are discussed. A detailed analysis of the surface behavior of the two faces in Cl^- free acid and alkaline solutions has also been carried out by cyclic voltammetry.

Keywords RuO_2 · Single crystal faces · Cl_2 evolution · Structure-activity relation

Introduction

The theory of electrocatalysis at oxide electrodes is doing its first steps [1, 2]. Thus far, phenomenological approaches have mainly been used essentially based on correlations where the parameter expressing the nature of the electrocatalyst is the energy change associated with some redox transition of the metal cation in the solid surface [3, 4]. The experimental data can however be hardly referred to the real surface area since electrocatalysts are as a rule prepared in the form of polycrystalline thin films whose stoichiometry is sometimes known as an average bulk value. Therefore, electronic and geometric effects cannot be separated to any extent.

Electrocatalysis at metal single crystals has been well developed, whereas the use of oxide single crystals has been very scanty thus far. In particular, in the case of RuO_2, besides some pioneering work in the early seventies [5, 6, 7], single crystal faces have been used to investigate oxygen evolution [8], potential of zero charge [9], hydrogen adsorption [10, 11], surface properties in solution [12, 13, 14] and in a vacuum [15, 16, 17], chlorine evolution and reduction [18, 19]. These studies have shown the presence of sizeable structural effects.

Polycrystalline surfaces and single crystal faces are at the two extremes of the scale of electrocatalytic activity. Apart from geometric effects, flat ordered surfaces are as a rule much less active than rough disordered surfaces. In the case of RuO_2, this has been proven for the reaction of O_2 evolution using the Tafel slope, an intensive quantity, which arranges electrocatalysts in order of increasing performance [20, 21]. In the end, the parameter expressing the structure of the electrocatalyst surface is particle size, expressed either as specific surface area in the case of supported Pt [22, 23], or as voltammetric charge in the case of RuO_2 layers [20, 24].

A different way to fill the gap between polycrystalline disordered surfaces and flat ordered faces is to look at stepped single crystal faces. In this way while the surface is still ordered, various kinds of active sites are introduced which characterize polycrystalline surfaces but whose precise structural features can be known and reproduced.

While such an approach is customarily pursued for metal surfaces not only in catalysis [25] but also in electrochemistry [26], nothing has been done thus far for oxide electrodes, in particular RuO_2. In the studies with RuO_2 single crystals only "as-grown" faces with low Miller indexes have been investigated, particularly the (110) face which is the most abundant natural face of tetragonal RuO_2 crystals. In this work we have used a natural (110) face and an artificial stepped surface, re-

Dedicated to Professor G. Horanyi on the occasion of his 70th birthday

E. Guerrini · V. Consonni · S. Trasatti (✉)
Department of Physical Chemistry and Electrochemistry,
University of Milan, Via Venezian 21,
Milan, 20133, Italy
E-mail: sergio.trasatti@unimi.it
Tel.: +39-02-50314223
Fax: +39-02-50314224

sulted to be (230), a vicinal surface only a bit off the natural (110) plane.

Chlorine evolution at polycrystalline oxide electrodes has been investigated extensively [27], but the details of the mechanism have been considerably modified over the years in correspondence with the disclosure of new experimental aspects. More specifically, the kinetics of chlorine evolution at RuO_2 anodes has turned out to be pH dependent which has suggested that at least one of the steps is probably common to the oxygen evolution reaction. The same has been found with Co_3O_4 and $NiCo_2O_4$ electrodes [19]. Since O_2 evolution is undoubtedly a ''demanding'' reaction on RuO_2 (which is revealed for instance by the increase of the Tafel slope as the oxide becomes more stoichiometric [21]) whereas Cl_2 evolution is apparently a ''facile'' reaction on the same surface, the possibility that the two processes can proceed through common steps is expected to diminish on the stoichiometric oxide. For the above reasons, it has been decided to investigate the effect of pH on the chlorine evolution reaction at RuO_2 single crystal faces as a very sensitive probe of the electrocatalytic activity of oxide surfaces. Previous study [18] has been carried out only by cyclic voltammetry at a single HCl concentration and the mechanism has been derived from the observed cathodic behavior of intermediates formed during the anodic discharge of chlorine ions.

Experimental

RuO_2 single crystals were grown by chemical vapor transport at the Brooklyn College as described elsewhere [28]. The crystal faces were identified by X-ray at the University of Illinois, Urbana; in particular, two (110) faces of sufficiently large size were selected and used. One of these $(1\bar{1}0)$ (the smaller one) was used as such, while the other was very gently mechanically polished. A successive X-ray analysis revealed that the exposed face was a $(\bar{2}\bar{3}0)$ plane, a vicinal surface very close to $(\bar{1}\bar{1}0)$. For the sake of simplification, the two surfaces will be referred to as (230) and (110), respectively.

The electrical contacts to the crystals were established by means of a flexible copper wire and conducting silver resin. The wire and the back of the crystal were then placed in an appropriate Teflon holder and the face to be investigated was finally isolated by means of suitable non-contaminating resins. In particular, the Schotchcast N. 4 resin used to mask Ag single crystals for double layer studies [29] has proved to be stable in strong acids and oxidants without unwanted interference on the experimental parameters.

The cell was the same as that described previously [8, 19]. Unless otherwise stated, solutions prepared using Millipore MilliQ grade water and analytical grade reagents were deaerated by bubbling purified N_2.

Surface characterization was carried out either in 0.5 mol dm^{-3} H_2SO_4 or 1 mol dm^{-3} KOH solutions. Chlorine evolution was studied in 5 mol dm^{-3} NaCl solutions containing 0.01 mol dm^{-3} HCl to keep the pH low.

The geometric surface areas of the electrodes were measured on photographic enlargements and were found to be 11.1 mm^2 for the (230) face and 4.5 mm^2 for the (110) face. No roughness factor corrections were introduced throughout in presenting experimental data (for the discussion of roughness factors see later text). The absolute values of the geometric surface areas may be subject to some uncertainty (especially at the crystal face edges), but the ratio between the two (which is more relevant here) is thought to deserve confidence.

Experiments were carried out potentiostatically in a water thermostat at 25 ± 0.1 °C. A saturated calomel electrode (SCE) was used in NaCl or KOH solutions, while a hydrogen electrode in the same solution (RHE) served as the reference electrode in H_2SO_4 solutions.

Results

Open circuit potential in Cl^- free solutions

On immersion, the open circuit potential has been measured to be around 0.95 V (rhe), a value similar to that observed with polycrystalline layers [30].

Voltammetric curves on the virgin crystal faces

Figure 1 shows the typical voltammetric curves of the two RuO_2 crystal faces in acid solutions. The curves appear to be somewhat more structured than observed previously with the crystals from the same source [12], while the qualitative features show some difference. Closer agreement is observed with Nagy et al.'s results [13], but the peak height ratio is lower in that work. Moreover, in both previous works [12, 13] voltammetric curves cover the whole potential window between H_2 and O_2 evolution. In this work the negative potential limit was 0.4 V (RHE) precisely to avoid any possible interference by the process of hydrogen adsorption/desorption.

The curves for the two faces are not dissimilar in general and only a closer inspection can reveal some specific differences. In particular, three pairs of peaks are observable with both faces, while only two are visible for (110) in previous studies [12, 13]. The peaks have been identified as A, B and C from the least to the most anodic one. Peak A appears to be slightly less reversible on the (230) face. For this reason, the anodic peak potential is somewhat more positive (ca. 0.78 V) on the (230) than on the (110) face (ca. 0.75 V).

Peak B is not well developed, but it is well reversible on both faces. Also the peak potential is the same at ca. 0.92 V (rhe). Peak C is much better developed. The potential is slightly more positive (1.28 V) on the (230) than on the (110) face (1.26 V). The reversibility is good on both faces. The apparent slight shift observed with the (230) face is thought to be essentially related to the steeper rise of the current at more anodic potentials.

Position and height of the peaks are not at all affected by the width of the potential range scanned during cycling. This is further evidence in favour of the reversibility of the surface reactions. Also, the potential sweep rate from 20 to 200 mV s^{-1} has been found not to modify the features of the curves.

The anodic and cathodic areas under peaks A and B are approximately the same, viz. the charges associated with the respective reactions are the same. The area under the anodic peak C is as a rule higher than that for the corresponding cathodic peak. This is thought to be due to the effect of the rising current at more anodic potentials. In particular, the anodic to cathodic charge ratio is higher for the (230) face, which suggests that the anodic process at more positive potentials has greater importance on this face.

Figure 2 shows the voltammetric curves in alkaline solution. The differences between the two faces are here striking. In particular, the curve for the (110) face exhibits the characteristic cathodic "tail" at low potentials already visible in a previous paper [12]. Moreover, peaks A and B have apparently merged into one peak A′, while a more anodic well developed peak C′ is still present; however the (110) face now shows a certain irreversibility of peak C′.

A closer inspection of the curves in Fig. 2 reveals that peak A′ is reversible on both faces, although a mismatch of about 20 mV can be recognized on the (110) face. The most intriguing aspect is that peak A′ is now at a less positive potential on (110) than on (230). In addition, the anodic peak C′ is now at more positive potentials with respect to Fig. 1, i.e. at 1.35 V for (230) and >1.4 for (110). The reduction peaks C′ are at ca. 1.32 V for both faces.

As in Fig. 1, the pairs of peaks A′ are almost symmetrical, which means that the anodic and cathodic

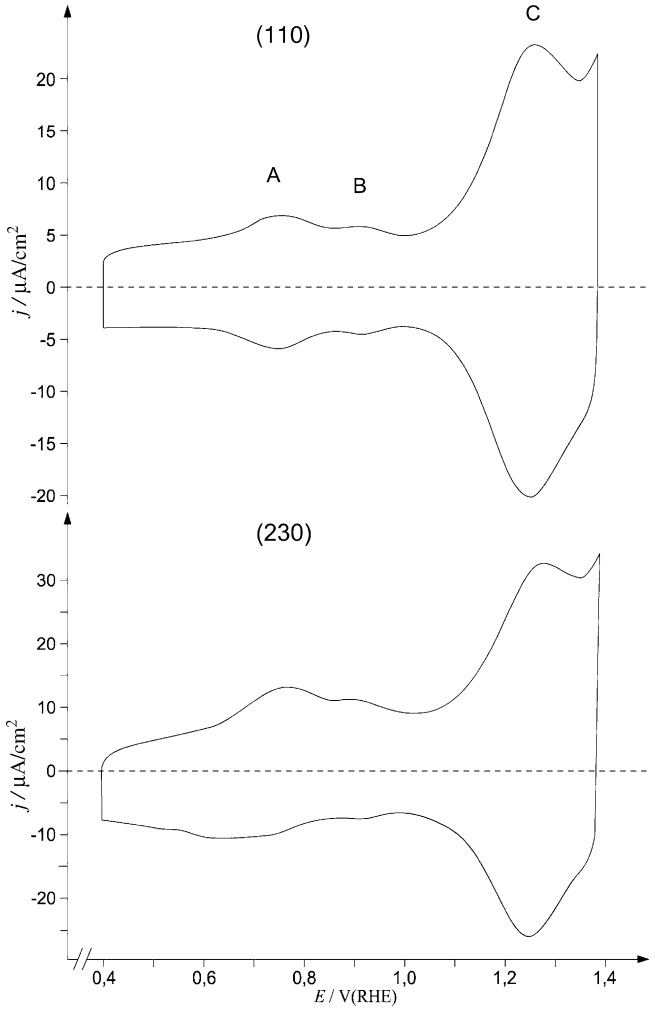

Fig. 1 Voltammetric curves at 100 mV s^{-1} of RuO_2 single crystal faces in 0.5 mol dm^{-3} H_2SO_4 solution

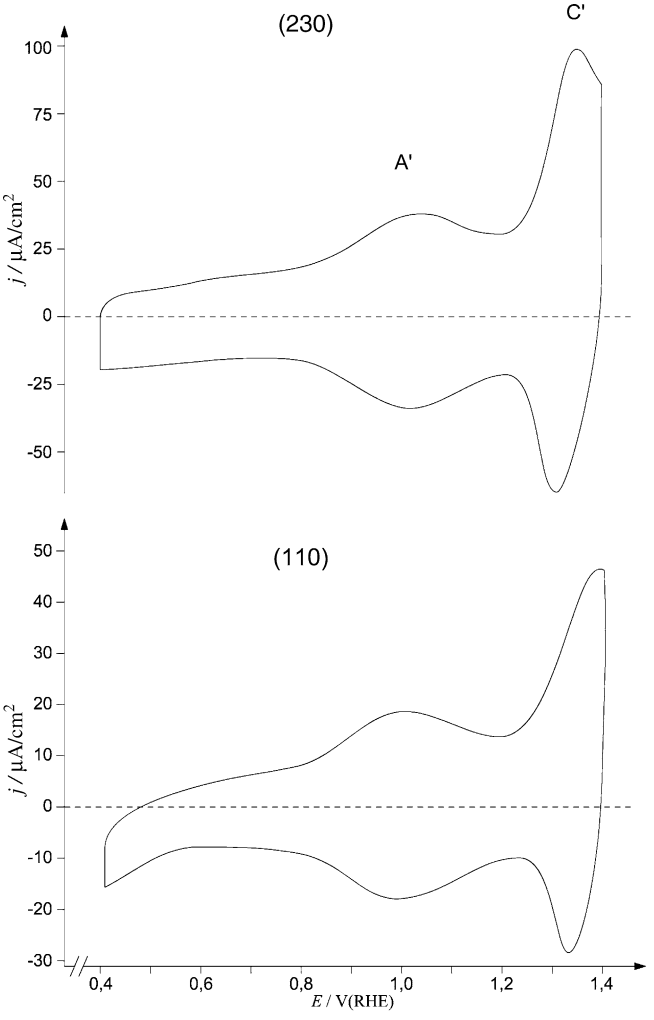

Fig. 2 Voltammetric curves at 100 mV s^{-1} of RuO_2 single crystal faces in 1.0 mol dm^{-3} KOH solution

charges are the same. Peaks C′ are again unbalanced. More specifically, the charge under peak C′ appears to be approximately twice that under peaks A′. On the contrary, in Fig. 1 the charge under peaks A + B is seen to be approximately equal to that under peaks C.

Tafel lines for chlorine evolution

Figures 3 and 4 show quasi-stationary potentiostatic curves for chlorine evolution from NaCl solutions at constant pH (ca. 0.9, by addition of HCl).

There are Tafel lines of 0.04 V extending over approximately two decades of current for the (230) face in 5 mol dm^{-3} NaCl. The Tafel line region is narrower for the (110) and becomes very short for both faces in 0.5 mol dm^{-3} NaCl. The deviations from the Tafel line are seen to depend on potential and not on current, which suggests that they are not related to uncompensated ohmic drops. The deviations commence at 1.10 V (SCE) for the (230) and at 1.14 V for the (110) face.

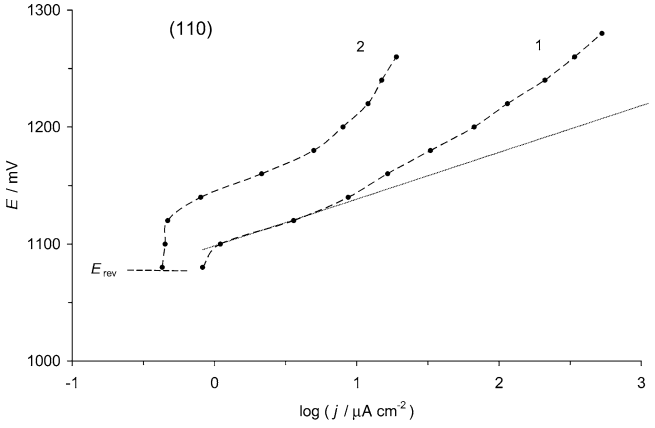

Fig. 3 Tafel plots for Cl_2 evolution on the (110) face of a RuO_2 single crystal. Solution: (1) 5 mol dm^{-3} NaCl; (2) 0.5 mol dm^{-3} NaCl. A concentration of 0.01 mol dm^{-3} of HCl is present in both cases. (.....) Slope of 40 mV. (- - - -) Theoretical reversible potential in the presence of 1% Cl_2 gas

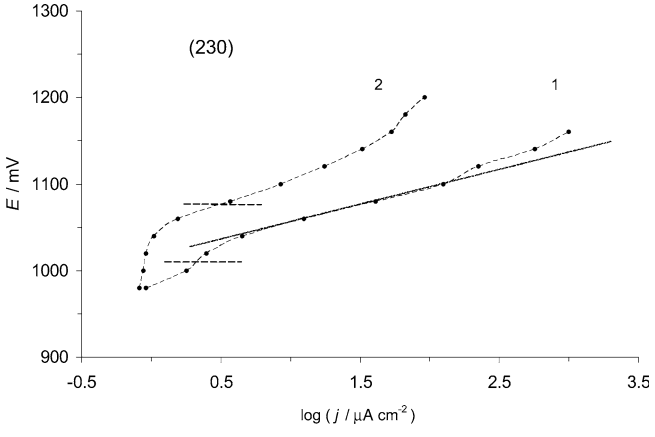

Fig. 4 Tafel plots for Cl_2 evolution on the (230) face of a RuO_2 single crystal. Solution: (1) 5 mol dm^{-3} NaCl; (2) 0.5 mol dm^{-3} NaCl. A concentration of 0.01 mol dm^{-3} of HCl is present in both cases. (.....) Slope of 40 mV. (- - - -) Theoretical reversible potential in the presence of 1% Cl_2 gas

The calculated reversible potentials of the Cl_2/Cl^- couple for a partial pressure of Cl_2 of 0.01 bar have been marked in the figures. These can only have qualitative significance since the solutions were purged with nitrogen during the experiments. However, it appears that chlorine evolution becomes appreciable at approximately the calculated reversible potential on the (230) face, whereas the start of the reaction is sensibly retarded on the (110) face. At constant current density, the difference in overpotential between the two faces is about 80 mV.

Orders of reaction for chlorine evolution

Figure 5 shows the dependence of the reaction rate at constant potential on the activity of Cl^- in the solution containing constantly 0.01 mol dm^{-3} HCl. As shown in a previous paper [19], the pH of the solution changes from about 2 to about 0.9 as the concentration of NaCl is increased. The plots show that the experimental points for the (230) face do not gather around a straight line. The reaction rate appears to be depressed the more the higher the NaCl concentration. This behavior resembles

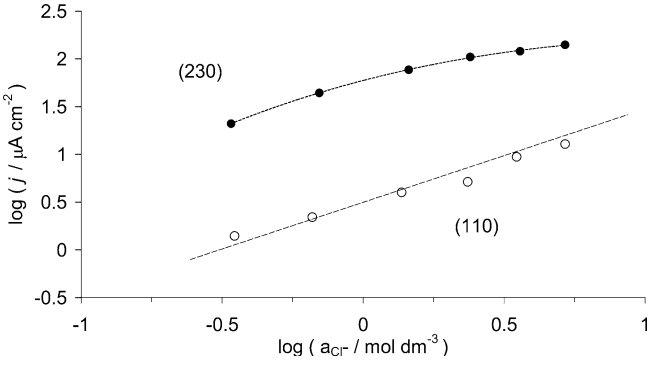

Fig. 5 Current density (j) versus log c_{NaCl} at constant HCl concentration (0.01 mol dm^{-3}). (230) plane, $E = 1.08$ V (SCE); (110) plane, $E = 1.14$ V (SCE). (—) Theoretical unit slope

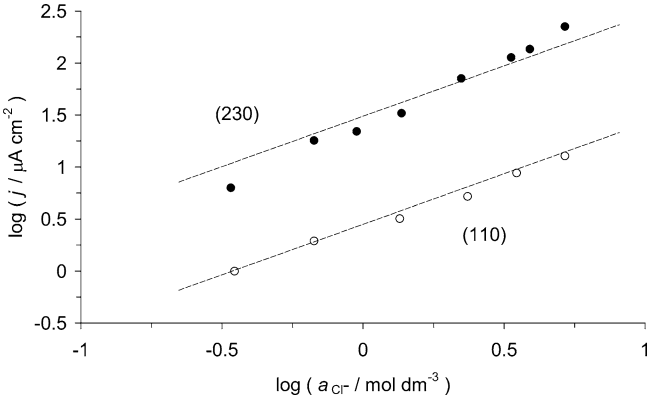

Fig. 6 Current density (j) versus log c_{NaCl} at constant pH. (230) plane, $E = 1.08$ V (SCE); (110) plane, $E = 1.14$ V (SCE). (—) Theoretical unit slope

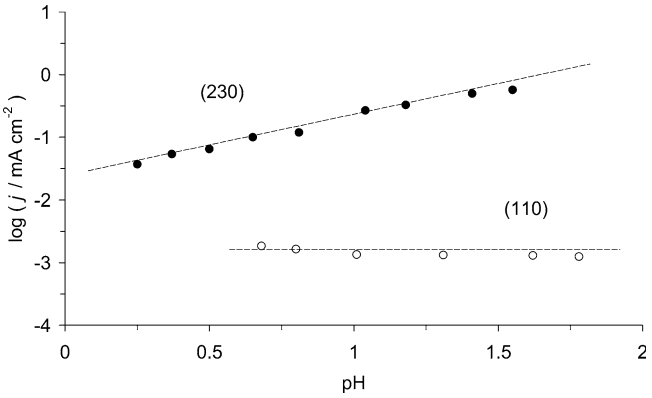

Fig. 7 Current density (j) versus pH at constant NaCl concentration. (230) plane, $E = 1.08$ V (SCE); (110) plane, $E = 1.14$ V (SCE). (—) Theoretical slopes of -1 and 0, for (230) and (110), respectively

that observed with polycrystalline samples [19, 31]. On the contrary, the points for the (110) face gather around a straight line of unit slope.

Figure 6 shows the same kind of data but taken keeping the pH of the solution constant by adding HCl where necessary. It has been verified that the additions do not interfere appreciably with the nominal concentration of chloride in solution. For both faces, the points now gather around a straight line of unit slope.

Figure 7 shows the dependence of the reaction rate of chlorine evolution at constant potential and constant NaCl concentration on the solution pH. While for the (110) face the reaction rate is to first approximation independent of pH, for the (230) face an order of reaction of -1 is observed, as reported for polycrystalline samples [19, 31]. Actually, a slight increase can be observed for (110) in the low pH range. Since any pH effect is expected to result in a depression of the reaction rate, the small enhancement observed is attributed simply to the slight increase in Cl^- concentration as a consequence of the addition of HCl to keep the pH constant.

Stoichiometric number for chlorine evolution

The theoretical reversible potential of the Cl_2/Cl^- couple was observed with both faces in the presence of Cl_2 gas. This allowed determining the stoichiometric number for the Cl_2 evolution reaction by comparing the "apparent" with the "actual" exchange current obtained via the charge transfer resistance and the extrapolation of the Tafel plots, respectively. The resulting stoichiometric number was found to be 1 within the experimental uncertainty.

Voltammetric curves on the used crystal faces

Immediately after extensive use in chlorine evolution, the voltammetric curve for the (110) face becomes featureless, more similar to that of polycrystalline samples. The original pattern is partly recovered long after the use in chloride solutions. However, the curves remain less structured although the relationships between the two faces are retained.

Discussion

Surface processes

As expected, the voltammetric curves of the single crystal faces show much better resolved features, yet qualitatively they do not differ substantially from those for polycrystalline electrodes. Under normal conditions, polycrystalline samples exhibit two broad humps, one centered around 0.8 V (RHE) and the other one around 1.3 V [21, 24, 32, 33]. With single crystal faces the first hump reveals the presence of a doublet, whereas the second hump becomes a resolved peak. Between the two regions, at about 1.0 V (rhe), there falls the open circuit potential. Therefore, the less positive peak is probably associated with the surface transformation of a more reduced species into RuO_2, while the more positive one corresponds to the conversion of RuO_2 into a more oxidized species.

The identification of the surface processes is not an easy task especially with single crystal faces since the lattice is not hydrated. This means that the metal–oxygen coordination number corresponds to that of the forming species only for the half of the metal surface complex towards the solution phase. For the rest the coordination number, especially towards the interior of the solid phase, is presumed to remain that typical of RuO_2, otherwise disruption and instability of the lattice should be observed. This is probably what happens at very anodic potentials where volatile RuO_4 is formed [34], but this is unlikely to be the case in the potential range before oxygen evolution.

The stoichiometry of the surface is difficult to assess. For both faces, the open circuit potential is that expected for RuO_2. This indicates that the surface Ru atoms towards the solution have saturated their coordination towards oxygen. Of course, the metal–oxygen binding energy of the surface bonds should differ from that for oxygen bridges between two Ru atoms in the interior of the lattice. It is therefore hard to expect that the observed peak potentials can have an exact correspondence in the Pourbaix diagrams [35] based on bulk phases.

Since the (110) face is expected to be largely present on polycrystalline samples, a certain parallelism might exist between the latter and single crystals. A quantitative investigation carried out by Doblhofer et al. [36] has suggested that one unit of charge is transferred to Ru ions between 0.4 and 1.0 V and one between 1.0 and 1.4 V (rhe). In other words, Ru(III) is present at 0.4 V, Ru(IV) at about 1.0 V and Ru(V) at ca. 1.4 V prior to oxygen evolution.

The above model is substantially supported by other authors' views [37–39] who proposed that O_2 evolution in acid solutions starts as the formation of RuO_3 commences, which implies that Ru(V) should be present on the surface at the potential of incipient oxygen evolution.

The nature of the doublet is unclear. Possibly, it could be associated with a surface rearrangement as the coverage with adsorbed species attains at a critical value. This rearrangement does not appear in the more anodic transition. The peak for the latter is narrower which suggests that lower lateral interaction between surface species should be involved.

The picture in the alkaline solution is markedly different and reflects the amphoteric nature of the RuO_2 surface. In addition, it should be recalled that the surface of RuO_2 possesses a strongly positive charge in acid solution and a strongly negative charge in alkaline solution [40, 41]. The energetics of the surface modifications can therefore be largely different.

If the assignment proposed by Burke and Murphy [37] is accepted, Ru(III) is present at 0.4 V (rhe) Ru(IV) at 0.8–0.9 V (rhe), Ru(VI) at about 1.2 V and Ru(VII) just prior to oxygen evolution. The Ru atoms are thus oxidised to a higher valency state in base. This is not surprising since, as found by Burke, the rate of change of the peak potentials with pH is higher than the classical Nernst value [42]. Therefore, the existence of a given oxidation state on the oxide surface is shifted to less positive potentials (with respect to RHE) as the pH is made more alkaline. As a consequence, states at higher valency than (V) are formed during oxygen evolution in acid but prior to it in base.

The presence of a smaller peak at the positive extreme of the potential range in alkaline solution has been observed also previously [43]. The anticipated formation of higher oxides in base reflects the higher chemical stability of these Ru compounds in alkaline solutions, i.e. it conforms to the known chemistry of Ru. At alkaline pH's the crystal faces show some more specific structural effects. Apart from the large cathodic "tail" for the (110) face already observed previously [12], the less positive potential of peak A′ for this face indicates stronger adsorption of intermediates. In other words, the surface shows a higher affinity for oxygenated species. This fact is probably also responsible for the higher irreversibility of peak C′. The formation of the species under this peak requires some more energy, but once formed are reduced at comparable potentials.

Although no specific investigation of O_2 evolution has been carried out in this work, the voltammetric curves can provide some hint of the relative activity of the two faces. In acid solution, oxygen evolution commences at about the same potential on both faces. This is in line with the fact that oxidation-reduction peaks fall at about the same potential. In alkaline solution oxygen evolution is presumably pushed to more positive potentials on the (110) face as a consequence of the higher difficulty to form Ru(VII) on this surface. As a result, this face appears to be less active, like for the electrocatalysis of oxygen evolution [8].

Surface charge

The assignment of the voltammetric peaks to various surface transitions requires consistency in the peak area ratio. Thus, peaks A + B (Ru III → IV) and peak C (Ru IV → V) are expected to have same area, which has actually been verified. Similarly, the area of peak A′ (Ru IV → VI) should be twice that of peak C′ (Ru VI → VII), which is in fact the case. As a whole, the charge measured in the potential range 0.4–1.4 V (rhe) in alkaline solution (Ru III → VII) should be twice that measured in acid solution (Ru III → V). Since the total (mean) charge (Q^*) for the (230) face has been found to be 32 μC in alkaline and 14 μC in acid solution, the ratio is actually close to 2 as expected. Similarly, for the (110) face the "alkaline" charge is 13.1 μC, while the "acid" one is 7.3. Thus, the ratio is again close to 2 (note that it is difficult to establish the precise correspondence of the potential range in acid and alkaline solutions).

"As-grown" surfaces look very flat on the microscope. If unit roughness factor is to a first approximation assumed for both faces, the charges for the two samples should be in the same ratio as their surface areas. For the acid solution, the (230)/(110) charge ratio is $R_{Q^*} = 3.8$ (the ratio for the alkaline solution does not lend itself to similar calculations because of the diversity of the voltammetric features). For the surface areas, $R_A = 2.5$. The difference is in principle attributable to the roughness of the (230) face (mechanically polished), with a plausible roughness factor of 1.5. The above conclusion is based on the assumption of the same Ru surface atom density on the two planes, that is difficult to assess for (230), but that can be reasonable in view of the small deviation of this plane from (110). It seems thus sound to conclude that the charge exchanged with the solution during surface redox transitions involves only surface metal ions (but see later on).

While on a relative basis the picture of surface charges appears self-consistent, it is more difficult to rationalize absolute quantitative aspects. With $n(110) = 1\times10^{15}$ cm^{-2} [10], q^* ($= Q^*/A$) should amount to 160 μC cm^{-2} for the exchange of one electron per surface metal ion. Therefore, the theoretical specific charge q^* should be 320 μC cm^{-2} in acid and 640 μC cm^{-2} in alkaline solution. In fact, the experimental q^*'s turn out to be almost exactly half the above values. The same is of course the case for the (230) face. The same observation is reported by Lister et al. [13], who however observed a very low peak at intermediate potentials (their peak A_3) so that the total charge exchanged between 0.4 and 1.4 V (RHE) is only ca. 95 μC cm^{-2} .

It is very intriguing to compare the above results with the findings of Burke et al. [44] who related the charge exchanged by a polycrystalline layer to the real surface area measured by the BET technique. According to their

calculations, one electron is exchanged every 0.08 nm^2 of real surface area as the electrodes are cycled between 0 and 1.4 V. Since the voltammetric curve for polycrystalline samples is almost featureless, the charge exchanged over a potential range of 1 V (like in this work) can be assumed to be $q^*/1.4$ that determined by Burke et al. Therefore, one electron ($=1.6\times10^{-19}$ C) is exchanged every $0.08\times1.4=0.115$ nm^2 of real surface area. Since the (110) face is the commonest in RuO_2 crystallites, it is acceptable to confront Burke's data with those for the (110) face in this work. Thus, $(7.3\times10^{-6}/1.6\times10^{-19})\,0.115\times10^{-14}=0.051$ cm^2, which differ by only ca. 14% from the measured geometric surface.

The above calculations can be questioned in principle on the ground that the BET surface area may not represent the actual working surface in electrochemical experiments. However, if the specific surface charge as found by Burke were too low, this would only mean that the BET technique gives a higher surface area. This is quite unlikely, since it has been shown that the BET surface area gives correct values at low surface area values but lower values (because of packing effects) at high surface area values [45]. The possibility that the BET value includes the surface area of regions not accessible to the solvent in wet experiments is to be ruled out on the basis of present evidence.

The surprising agreement between the specific value of q^* found here (about 0.16 mC cm^{-2} real surface area) and that proposed on the basis of polycrystalline RuO_2 (about 0.14 mC cm^{-2} BET surface area) breaks down in alkaline solution. In fact, q^* has been found to remain the same for polycrystalline samples, whereas it becomes twice as much for single crystal faces. On the other hand, the doubling of the current in alkaline solution can be observed also in the voltammetric curves of previous papers for all faces investigated [12, 13]. This particular aspect requires further investigation.

Time-dependent surface charge

Voltammetric charge has been shown to depend on the potential scan rate for polycrystalline RuO_2 [32]. This effect has been attributed to the slow penetration of protons along defective paths, such as cracks, pores, grain boundaries, etc. In principle, such an effect should be absent with single crystal faces without morphological defects. Figure 8 shows that this is in fact not the case.

The voltammetric charge was determined as a function of the potential scan rate (v) in a very narrow potential range between 0.4 and 0.5 V (SCE), away from visible peaks. v was varied from 10 to 100 mV s^{-1}. Figure 8 shows unambiguously that q^* depends on the scan rate, more appreciably for the (230) than for the (110) face. This indicates that even with single crystals there is a slow process governing the exchange of protons between the oxide surface and the adjacent solution layer [14].

In previous papers, one of us has shown [46, 47] that q^* can be extrapolated to $v \to 0$ as well as to $v \to \infty$. The former extrapolation gives the total charge q_t^* while the latter gives the outer voltammetric charge q_o^*. Figure 9 shows the extrapolation to $v=0$. q_t^* results to be 20 μC cm^{-2} for (110) and 42 μC cm^{-2} for (230). The charge ratio 2.1 turns out slightly higher that 1.5 resulting at 100 mV s^{-1} (cf. Fig. 1). The higher ratio at $v=0$ is probably more representative of the actual surface roughness of the (230) face.

Figure 10 shows the extrapolation of the voltammetric charge to $v=\infty$. q_o^* is 54 μC cm^{-2} for (230) and 76 μC cm^{-2} for (110). The outer charge turns out surprisingly higher for (110) than for (230).

The dependence of q^* on v for single crystal faces entails that there is a diffusional component in the process of site oxidation/reduction even on as flat a surface as a perfect (110) face. This process does not necessarily involve the penetration of protons into the lattice. It can also be related to the motion of molecular groups in the transition of proton from water (hydronium ions) to OH groups on the solid surface. This view is corroborated by the observation that the ratio q_t^*/q^* (q^* is the charge at 100 mV s^{-1}) is only two for the (110) face. Since q^* has been found to involve only about 50% of the Ru surface sites, q_t^* corresponds to the involvement of 100% of the sites. If q_t^* included proton

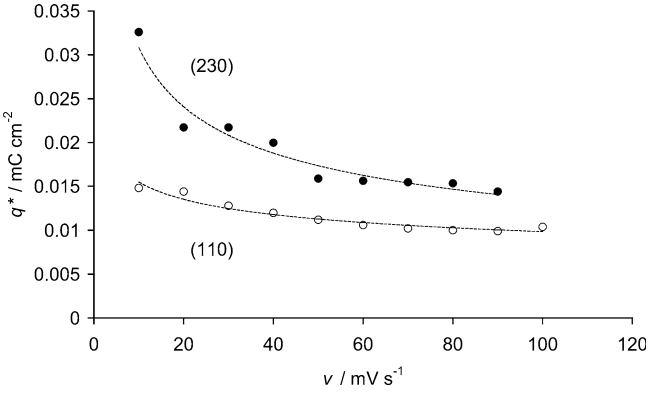

Fig. 8 Dependence of the voltammetric charge between 0.4 and 0.5 V (SCE) on the potential scan rate

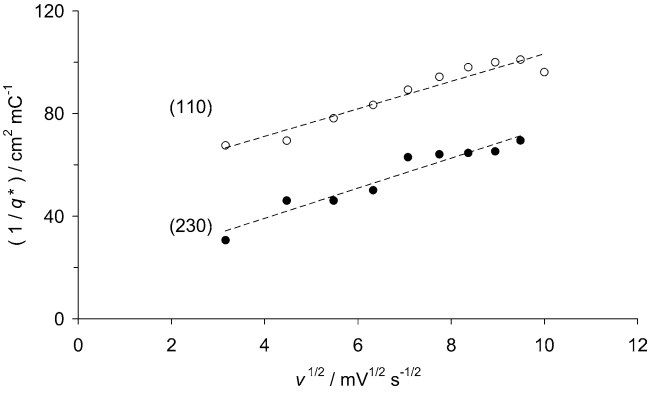

Fig. 9 Extrapolation of the charge in Fig. 8 to the potential scan rate $v=0$

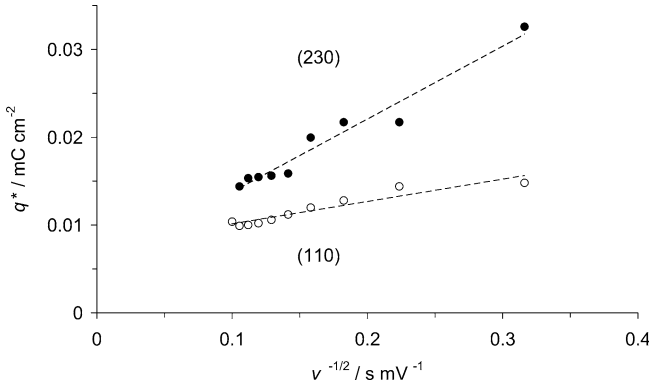

Fig. 10 Extrapolation of the charge in Fig. 8 to the potential scan rate $v = \infty$

penetration into the lattice, its value would be expected to be much higher.

The situation is more complex for the (230) face. Data show that the ratio q_t^*/q^* is higher than two and especially that q_o^* becomes lower than that for the (110). This can only imply that the diffusional component during a voltammetric scan is more important the more open the surface structure. In other words, the (230) surface is likely to contain sites that are kinetically more difficult to reach and are thus excluded as $v \to \infty$.

Mechanism of chlorine evolution

The experimental kinetic parameters of the anodic reaction of chlorine evolution are unambiguous. The Tafel slope is 40 mV for both crystal faces. This indicates that the rate-determining step involves the second electron transfer. Since the stoichiometric number has been found to be 1, of the classical mechanisms only that involving the ion + atom step ($Cl^- + Cl$) would be plausible. However, such mechanism would require an order of reaction of two with respect to Cl^-, which is not the case. Once again, the parameters of Cl_2 evolution on oxides prove that the classical mechanisms are unsuitable to explain the experimental picture [27].

The order of reaction of one with respect to Cl^- indicates that this species appears only once in the steps up to the rate determining one included. The order of reaction of zero with respect to protons for the (110) face rules out that the mechanism can include a step whose potential shifts with pH. Therefore, the mechanism of chlorine evolution on the (110) face of RuO_2 single crystals is basically different from that on polycrystalline layers although the main parameters have the same values. The only mechanism that appears to be reasonable is thus the earlier one proposed by Krishtalik and co-workers [48], i.e.:

$$S + Cl^- \leftrightarrow S - Cl + e \quad (2a)$$

$$S - Cl \rightarrow (S - Cl)^+ + e \quad \text{rds} \quad (2b)$$

$$(S\text{--}Cl)^+ \ldots \leftrightarrow Cl_2 \quad (2c)$$

where S is a surface active site whose precise nature is unknown. But it is realistic to assume that the core of the active site is the Ru ion.

The reason why any pH dependence is absent is to be sought in the especially high overpotential for O_2 evolution [8] compared to that for Cl_2 evolution on the (110) face. The surface reaction of site oxidation preceding O_2 generation is probably pushed to higher potentials on the (110) face. The relative activity of the catalyst surface for O_2 versus Cl_2 evolution is thought to be responsible for the appearance or not of the pH dependence of Cl_2 evolution [49]. The intrinsic redox behavior of the surface active sites provides the ability for them to draw two electrons from the same discharging species as an alternative to the classical ion + atom ($Cl + Cl^-$) step.

The mechanism on the (230) face appears to differ from that on the flat (110) face, being closer to that on a polycrystalline surface [19]. In this case, the order of reaction of −1 with respect to protons calls for a surface oxidation step preceding Cl^- discharge [50, 51]:

$$S\text{--}OH \rightarrow S\text{--}O + H^+ + e \quad (3a)$$

$$S - O + CL^- \rightarrow S - OCL + e \quad \text{rds} \quad (3b)$$

$$S - OCl + H^+ + Cl^- \rightarrow S - OH + Cl_2 \quad (3c)$$

The experimental Tafel slope of 40 mV points to Eq. 3b as the rate determining step. Therefore, the precise nature of step Eq. 3c is not important since it follows the rds.

The (110) face is clearly less active than the (230) face. In terms of the proposed mechanism, this implies that either S–Cl is at lower energy or $(S\text{–}Cl)^+$ is at higher energy. Both situations probably occur on the (110) face at the same time. The S–Cl bond strength is presumably higher because of the large number of unsaturated surface bonds; on the other hand, due to the compactness of the atom distribution, the lateral interaction between two neighboring $(S\text{–}Cl)^+$ species is stronger. The absence of any pH effect also on the (110) face suggests that both O_2 and Cl_2 evolution are inhibited on this face compared to the (230) face. It has to be concluded that the dramatic activation of the (230) with respect to the (110) face, despite they are structurally vicinal, is related to the more favorable interaction of the intermediates with "oxygenated" surface sites. In other words, the activation of the surface towards O_2 evolution, related to the more open structure of (230), is responsible for the activation of the same surface towards Cl_2 evolution.

The deviation from the Tafel line of 0.04 V slope at more anodic potentials (cf. Figs. 3 and 4) cannot be related to ohmic drop effects because of the high conductivity of the single crystals and the small current circulating in the cell. It is possible that either the rate-determining step shifts to the primary discharge (Eqs. 2a and 3a) or the oxygen evolution reaction starts to interfere with the Cl_2 evolution process in the high

overpotential range. With polycrystalline samples, the Tafel slope has been found to stay constant for many decades of current [19, 52]. Thus, the second possibility is more realistic. If this is the case, the kinetic parameters should change in the high overpotential range; in particular, some sort of pH dependence should appear also for the (110) face. The verification of this hypothesis requires further experimental study.

At constant potential on the linear part of the Tafel plots, the ratio of current density, j, is (230)/(110) = 130. If the same atomic density were assumed for both faces, the activity ratio, corrected for the roughness factor of (230) becomes 87. Since the real atom density on (230) is probably lower than that on (110), the (230) plane turns out to be more active that the (110) plane by ca. two orders of magnitude. This can only be explained in terms of real electrocatalytic effects. The higher activity of the (230) plane is to be related to its more open structure as well as to the presence of atoms with unsaturated surface bonds which can interact more favorably with reactants, intermediates, and/or products of the reaction.

The voltammetric curves become less structured after extensive use of the electrodes in Cl_2 evolution. However, the relative features of the two faces are apparently retained. Immediately after prolonged discharge of Cl_2, the curves are even more distorted. This indicates that a sort of ''atom implantation'' takes place during the discharge of Cl^- ions, which deteriorates the surface response. The voltammetric ''spectrum'' thus becomes more like that of polycrystalline layers. The penetration of chlorine into the oxide layer has been observed with thermal oxides [53]. However, in that case grain boundary diffusion is probably responsible for the observed phenomenon. Penetration should not take place on single crystal faces, but the surface is anyway appreciably disturbed. Further surface studies are needed to gain insight into this particular aspect.

Conclusions

This work has revealed for the surface and electrocatalytic behavior of RuO_2 single crystal faces aspects not pointed out before.

(1) A (230) plane, a vicinal surface of (110), has been investigated for the first time. Despite the close similarity of the voltammetric pattern, the electrocatalytic activity is dramatically different. In particular, pH effects are not observed with (110) while they are substantial with (230).

(2) The electrocatalytic activity for Cl_2 evolution does not appear to be related to the chemical composition of the surface, but rather to its morphology. A (230) surface, more open than (110), shows a higher activity for Cl_2 evolution thanks to its easier oxidisability. Thus, surface oxidation is a prerequisite for low overpotential for Cl_2 evolution. The structure of the surface complex is the key to the electrocatalytic activity of RuO_2.

(3) The (110) face of RuO_2 exchanges one electron per Ru surface atom in the potential range 0.4–1.4 V (RHE). In the same range the valency state of Ru atoms is expected to change from III to V. Thus, only half of the surface atoms are normally involved. If the potential scan rate is reduced to zero (i.e., the rate of surface processes), the atoms involved turn out to become 100%. This indicates that the exchange of protons between oxide surface and solution adlayer is limited by a diffusional component even for single crystal faces. The diffusional component is thought to be related to local motion of molecular groups (H_3O^+ and surface OH), and not to penetration of protons into the crystal lattice.

(4) The surface voltammetric charge doubles in alkaline solution with respect to the value in acid solution. This agrees with a higher valency state of Ru atoms in alkaline solution, so that in the 0.4–1.4 V (RHE) potential range the transition is III–VII compared with III–V in acids. The involvement of only half of the surface atoms in ordinary conditions persists also in alkaline solution.

Acknowledgements The authors are grateful to the Italian National Research Center (CNR, Rome) and to MIUR (CoFin) for financial support to this work.

References

1. Liu P, Logadottir A, Nørskov JK (2003) Electrochim Acta 48:3731
2. Anderson AB (2003) Electrochim Acta 48:3743
3. Tseung ACC, Jasem S (1977) Electrochim Acta 22:31
4. Trasatti S (1980) J Electroanal Cem 111:125
5. Trasatti S, Buzzanca G (1971) J Electroanal Chem 29A:1
6. Horkans J, Shafer MW (1977) J Electrochem Soc 124:1202
7. Schäfer R, Grofe T, Trenkel M (1973) J Solid State Chem 8:14
8. Castelli P, Trasatti S, Pollak FH, O'Grady WE (1986) J Electroanal Chem 210:189
9. Tomkiewicz M, Huang YS, Pollak FH (1983) J Electrochem Soc 130:1514
10. Hepel T, Pollak FH, O'Grady WE (1984) J Electrochem Soc 131:2094
11. Lister TE, Tolmachev YV, Chu Y, Cullen WG, You H, Yonco R, Nagy Z (2003) J Electroanal Chem 554–555:71
12. O'Grady WE, Goel AK, Pollak FH, Park HL, Huang YS (1983) J Electroanal Chem 151:295
13. Lister TE, Chu Y, Cullen W, You H, Yonco RM, Mitchell JF, Nagy Z (2002) J Electroanal Chem 524–525:201
14. Doubova LM, Daolio S, De Battisti A (2002) J Electroanal Chem 532:25
15. Atanasoska LJ, O'Grady WE, Atanasoski RT, Pollak FH (1988) Surf Sci 202:142
16. Atanasoska LJ, O'Grady WE, Pollak FH, Atanasoski RT (1990) Surf Sci 230:95
17. Basame SB, Habel-Rodriguez D, Keller DJ (2001) Appl Surf Sci 183:62
18. Hepel T, Pollak FH, O'Grady WE (1986) J Electrochem Soc 133:69
19. Consonni V, Trasatti S, Pollack F, O'Grady WE (1987) J Electroanal Chem 228:393
20. Angelinetta C, Trasatti S, Atanasoska LJD, Minevski ZS, Atanasoski RT (1989) Mater Chem Phys 22:231

21. Trasatti S (1994) Transition metal oxides: versatile materials for electrocatalysis. In: Lipkowski J, Ross PN (eds) The electrochemistry of novel materials. VCH Publishers Inc., New York, pp 207–295
22. Bagotzky VS, Skundin AM (1984) Electrochim Acta 29:757
23. Trasatti S (1992) Electrocatalysis of hydrogen evolution: progress in cathode activation. In: Gerischer H, Tobias CW (eds) Advances in electrochemical science and engineering. VCH, Weinheim, pp 1–85
24. Trasatti S (1990) Electrochim Acta 36:225
25. McCrea KR, Parker JS, Somorjai GA (2002) J Phys Chem B 106:10854
26. Attard GA, Hazzazi O, Wells PB, Climent V, Herrero E, Feliu JM (2004) J Electroanal Chem 568:329
27. Trasatti S (1987) Electrochim Acta 32:369
28. Huang YS, Park HL, Pollak FH (1982) Mater Res Bull 17:1305
29. Bacchetta M, Trasatti S, Doubova L, Hamelin A (1986) J Electroanal Chem 200:389
30. Galizzioli D, Tantardini F, Trasatti S (1974) J Appl Electrochem 4:57
31. Trasatti S (1992) Hydrogen evolution on oxide electrodes. In: Wellington TC (ed) Modern chlor-alkali technology. Elsevier Applied Science, Amsterdam, pp 281–294
32. Trasatti S, Lodi G (1980) Properties of conductive transition metal oxides with rutile-type structure. In: Trasatti S (ed) Electrodes of conductive metallic oxides, part A. Elsevier, Amsterdam, pp 301–358
33. Trasatti S (1999) Interfacial electrochemistry of conductive oxides for electrocatalysis. In: Wieckowski A (ed) Interfacial electrochemistry. Marcel Dekker, New York, pp 769–792
34. Kötz R, Stucki S, Scherson D, Kolb DM (1984) J Electroanal Chem 172:211
35. Pourbaix M (1974) Atlas of electrochemical equilibria in aqueous solutions. NACE, Houston, pp 343–349
36. Doblhofer K, Metikos M, Ogumi Z, Gerischer H (1978) Ber Bunsenges Phys Chem 82:1046
37. Burke LD, Murphy OJ, O'Neill JF, Venkatesan S (1977) JCS Faraday I 73:1659
38. Rasiyah P, Tseung ACC (1984) J Electrochem Soc 131:803
39. Lodi G, Sivieri E, De Battisti A, Trasatti S (1978) J Appl Electrochem 8:135
40. Ardizzone S, Trasatti S (1996) Colloid Interface Sci 64:173
41. Ardizzone S, Siviglia P, Trasatti S (1981) J Electroanal Chem 122:395
42. Burke LD, Whelan DP (1981) J Electroanal Chem 124:333
43. O'Grady WE, Iwakura C, Huang J, Yeager C (1974) In: Breiter MW (ed) Electrocatalysis. Electrochem Soc, Princeton, pp 286–297
44. Burke LD, Murphy OJ, O'Neill JF (1977) J Electroanal Chem 81:391
45. Trasatti S, Petrii OA (1991) Pure Appl Chem 63:711
46. Ardizzone S, Fregonara G, Trasatti S (1990) Electrochim Acta 35:263
47. Baronetto D, Krstajic N, Trasatti S (1994) Electrochim Acta 39:2359
48. Erenburg RG, Krishtalik LI, Bystrov VI (1972) Elektrokhimiya 8:1740
49. Trasatti S, Lodi G (1981) Oxygen and chlorine evolution at conductive metallic oxide anodes. In: Trasatti S (ed) Electrodes of conductive metallic oxides, part B. Elsevier, Amsterdam, pp 521–626
50. Erenburg RG (1984) Elektrokhimiya 20:1602
51. Krishtalik LI (1981) Electrochim Acta 26:329
52. Ardizzone S, Carugati A, Lodi G, Trasatti S (1982) J Electrochem Soc 129:1689
53. Augustinsky J, Balsenc L, Hinden J (1978) J Electrochem Soc 125:1093